Title: A Diminished North Atlantic Nutrient Stream during Younger Dryas Climate Reversal

Authors: Jean Lynch-Stieglitz[1]*, Tyler D. Vollmer[1], Shannon G. Valley[1], Eric Blackmon[1], Sifan Gu[2], Thomas M. Marchitto[3]

Affiliations:

[1]School of Earth and Atmospheric Sciences, Georgia Institute of Technology; Atlanta GA 30332, USA

[2]School of Oceanography, Shanghai Jiao Tong University, Shanghai, People's Republic of China

[3]INSTAAR, University of Colorado, Boulder, CO, USA

*Corresponding author. Email: jean@eas.gatech.edu

Abstract: The high rate of biological productivity in the North Atlantic is stimulated by the advective supply of nutrients into the region via the Gulf Stream (nutrient stream). It has been proposed that the projected future decline in the Atlantic Meridional Overturning Circulation (AMOC) will cause a reduction in nutrient supply and resulting productivity. Here we examine how the nutrient stream changed over the Younger Dryas climate reversal that marked the transition out of the last ice age. Gulf Stream nutrient content decreased, and oxygen content increased at the Florida Straits during this time of weakened AMOC. The decreased nutrient stream was accompanied by a reduction in biological productivity at higher latitudes in the North Atlantic, supporting the link postulated in theoretical and modelling studies.

One-Sentence Summary: Paleoceanographic data supports hypothesis linking delivery of nutrients by Gulf Stream to high latitude productivity.

Main Text:

The Gulf Stream and North Atlantic Drift serve as a northward flowing conduit of nutrient-rich intermediate waters (*1, 2*). In the subpolar North Atlantic the density surfaces bearing these nutrients shoal and the nutrients are incorporated into the deep winter mixed layer (*3*). During the spring bloom these nutrients drive primary productivity in the sunlit surface ocean. The high nutrient waters of the Gulf Stream have been termed the "nutrient stream" and this advective pathway is thought to be the dominant source of nutrients supporting phytoplankton productivity in the subpolar North Atlantic (*4, 5*). The Gulf Stream originates in the Florida Straits and as it moves northward along the western boundary of the subtropical gyre, both the mass and nutrient transport of the current is augmented by recirculating water within the North Atlantic basin. However, the ultimate source of the nutrients to the incipient Gulf Stream in the Florida Straits is the import of high nutrient intermediate-depth waters from the tropics, which are replenished by the high-nutrient Southern Hemisphere intermediate and mode waters as part of the upper (northward) limb of the Atlantic Meridional Overturning Circulation (AMOC) (*2, 6*). In addition to supplying the nutrient stream, the Southern Hemisphere intermediate and mode waters supply the nutrients that drive much of the primary production at low and mid latitudes (*7, 8*).

The AMOC is projected to weaken over the coming century with the increase in anthropogenic greenhouse gasses (*9*). Consequently, the nutrient stream is projected to weaken, leading to basin scale changes in biogeochemistry and decreased primary production. Declines in primary production would impact the important North Atlantic fisheries, and may also impact the uptake of anthropogenic CO_2. While a future decline in North Atlantic export production under future warming scenarios has long been projected (*10*), it has only more recently been recognized that the decline in the nutrient stream is the dominant mechanism driving this change (*11*). Whitt (*5*) found that, when driven with the high emissions RCP8.5 scenario, the Community Earth System Model (CESM) shows a 35% decline in Gulf Stream nitrate transport at 30°N in 2080 in response to a 39% decline in AMOC and find that the decreased nutrient stream is the primary driver of the associated decline in North Atlantic export productivity. Tagklis et al. (*12*) showed that the weakening of AMOC over the next century in the multi-model mean of seven CMIP5 models results in reduced upper-ocean phosphate concentration, upper-ocean apparent oxygen utilization, and primary productivity in the North Atlantic, and they attribute these changes to the decreased nutrient stream. Using biogeochemical data from an ice core, Osman et al. (*13*) reconstructed a decline in North Atlantic primary productivity over the industrial era, which they attributed to a weakening AMOC. There are multiple lines of evidence that the AMOC weakened during the Younger Dryas cold interval that punctuated the transition out of the last ice age (*14*). In this paper we assess the link between the AMOC and nutrient stream for the Younger Dryas event through the reconstruction of nutrient and oxygen concentrations in the deepest waters of the Florida Straits and explore the consequences for North Atlantic productivity. While the details of the background climate state and time scale of change differ from the present day, this past climate event provides an opportunity to test the mechanisms that have been identified in the climate models.

Reconstruction of Seawater Biogeochemistry in the Florida Straits

Sediment core KNR166-2-26JPC was recovered from 24°19.61'N, 83°15.14'W in the Florida Straits at 546 m water depth. Due to the high sedimentation rates, this core provides exceptional time resolution over the Younger Dryas climate reversal. The coring site along the Florida margin is currently bathed by Antarctic Intermediate Water (AAIW) (potential density = 27.3 kg m^{-3}), which at this location is characterized by high nutrient and low oxygen concentrations and supplies new nutrients to the North Atlantic (*2, 6*) (**Fig. 1**). In this paper we reconstruct seawater dissolved oxygen concentration at this location using carbon isotope measurements in paired epifaunal and deep infaunal benthic foraminifera, following an approach pioneered by McCorkle and Emerson (*15, 16*). *Planulina ariminensis* occupies a habitat on top of the sediments and records seawater $\delta^{13}C$ values, and *Globobulimina* has a habitat deep within the sediments where the dissolved carbon has much lower $\delta^{13}C$ values and oxygen is reduced to near zero values from the respiration of organic matter within the sediments. The difference between the $\delta^{13}C$ values in the tests of these two benthic foraminifera is used to quantitatively reconstruct past oxygen concentrations (*17*). We also present abundance data for three thermocline dwelling species of planktonic foraminifera which are currently abundant in areas with subsurface low oxygen layers, *Globorotalia menardii, Globorotalia tumida, and Pullentina obliquiloculata (18)*. At this location, we have previously published Cd/Ca measurements in benthic foraminifera which were used to reconstruct changes in seawater Cd_w, which mimics the distribution of the major nutrient PO_4 in the ocean (*19*). We have also published benthic foraminiferal Mg/Li (*20*) to reconstruct temperature at this site over the deglaciation. We also use a previously published age model for this core (*21*). We estimate past PO_4 concentrations, using the Cd_w reconstructions, and Apparent Oxygen Utilization (AOU), a measure of oxygen consumption in the subsurface ocean that is determined from the difference between in-situ and saturation oxygen concentration, using the quantitative temperature and oxygen reconstructions. We then use the PO_4 and AOU to estimate separately changes in the PO_4 concentration inherited from the source regions (preformed PO_4, P_{pre}) and the PO_4 that has been contributed to the subsurface from the remineralization of organic matter. Because intermediate waters leave the surface slightly undersaturated in oxygen, AOU overestimates true subsurface oxygen utilization, and P_{pre} can be underestimated by up to 0.2 μM, depending on the climate state. Detailed methods can be found in the Supplementary Information.

Weakened Florida Straits Nutrient Stream during the Younger Dryas

While the intermediate waters that supply the nutrient stream have high PO_4 and oxygen concentrations (high P_{pre}, low AOU) when they leave the surface in the Southern Hemisphere, these properties change as the waters transit northward through the tropics. Export productivity from overlying surface waters adds PO_4 and consumes O_2 via the oxidation and remineralization of sinking organic matter. Since the productivity is itself fed by a continuous supply of preformed nutrients, the accumulation of remineralized PO_4 and depletion of oxygen both depend on the northward flow of nutrient-charged intermediate waters (*22*). As the AMOC weakened during the Younger Dryas (*14*), this contribution of nutrient-rich, low oxygen intermediate water from the south would have diminished, replaced by lower PO_4 and higher oxygen intermediate waters formed locally in the North Atlantic. We therefore would expect an increase in the oxygen concentrations in the deep Florida Straits. Indeed, we reconstruct high oxygen values during the Younger Dryas from the dual carbon isotope approach, and increased oxygenation of the waters in the Florida Straits is also supported by the disappearance of the planktonic foraminifera *G. menardii, G. tumida*, and *P. obliquiloculata* (**Fig. 2**). The small

warming of the waters transiting the site of about 2°C during the Younger Dryas interval (*20*) would imply a decrease in oxygen concentration at saturation with the atmosphere, and the decrease in AOU is consequently slightly larger than the increase in oxygen. This is, again, what is expected if the oxygen increase is driven by the diminished contribution of the high AOU intermediate waters from the tropics.

A more direct measure of the nutrient stream comes from estimates of the concentration of the major nutrient PO_4 in the deep Florida Straits (**Fig. 3**). This estimate is based on the Cd/Ca in *H. elegans*, a different species of benthic foraminifera than was used to reconstruct oxygen via the carbon isotope measurements. The PO_4 at this site reflects contributions of intermediate waters formed in both hemispheres, including the regenerated PO_4 from the remineralization of organic matter in the tropics. We find a strong Younger Dryas decrease in PO_4 and, given that the intermediate water Northern and Southern end member values did not change by much over this time period (**Fig. S2b**), the lower PO_4 in the Florida Straits is consistent with the weakened AMOC. To probe this further, we use the AOU to separate the PO_4 concentration into its preformed (P_{pre}) and regenerated ($PO_4 - P_{pre}$) components. The PO_4 reduction primarily reflects a small decrease in P_{pre}, and a much larger decrease in the regenerated PO_4, as inferred from the large AOU decrease (**Fig. 3**). Today the intermediate waters formed in the Southern Hemisphere have a higher P_{pre} than those that form in the North Atlantic, so a lower P_{pre} is expected during a time of weakened AMOC when a larger proportion of Northern Hemisphere sourced intermediate waters would have bathed the site. Similarly, with a weakened AMOC we expect a lesser contribution of intermediate waters that have transited through the tropics, where they gain a high regenerated PO_4 content. There may have also been a positive feedback whereby the reduced northward transport of nutrients led to less productivity and remineralization in the tropics. The reduction of both pre-formed and regenerated PO_4 throughout the intermediate-depth North Atlantic, coupled with a decreased contribution of intermediate waters from the Southern Hemisphere, is also inferred for the Last Glacial Maximum, based on an inversion of the spatially more extensive data-set for that time period (*23*).

Biogeochemical Consequences of a Weakened vs. Collapsed AMOC

While it has been established that the surface branch of the AMOC replenishes the modern nutrient stream, and that a future century-scale weakening of the AMOC will result in a weaker nutrient stream and lower North Atlantic productivity, it is not immediately apparent that these concepts and expectations translate directly to the Younger Dryas, a millennial scale event that occurred on the deglaciation. Schmittner (*24*) simulated a millennial scale AMOC collapse and recovery using freshwater forcing in an intermediate complexity model. While a productivity decline is observed, the mechanism behind this decline under a collapsed AMOC differs from the simulations for a future weakening of the AMOC. The decline in productivity in this case is attributed to strong near-surface density stratification, and the intermediate water nutrient content in the upper 1 km of the North Atlantic is higher over the duration of the shutdown rather than lower as in the future scenarios. Another set of equilibrium experiments under Last Glacial Maximum boundary conditions in a different intermediate complexity model confirmed this behavior for a simulation where the large scale AMOC is completely collapsed due to strong freshwater forcing (*25*). However, when AMOC is weakened, but not shut down completely, the PO_4 in the upper 2 km of the North Atlantic is lower than the control state, consistent with the pattern seen for the future transient (*12*) and in our reconstruction for the Younger Dryas. The transient response of a long paleoclimate simulation using CESM1 (*26*) can be used to explore

the relationship between AMOC, biogeochemical properties in the upper North Atlantic, and productivity. In this simulation, as the AMOC and nutrient stream weaken, the nutrient content of the upper North Atlantic and primary productivity both decline (**Fig. S2a**). However, when the AMOC is almost absent, a state with low productivity and *high* open ocean North Atlantic intermediate water nutrient content is seen, as in the AMOC collapse scenarios of the intermediate complexity models. The intermediate water Cd_w records in the Florida Straits and in the open ocean North Atlantic converge at low values during the Younger Dryas, consistent with what the model shows for a very weak AMOC and diminished nutrient stream, but not a fresh-water induced collapse (**Fig. S2b**).

Impact of Weakened Younger Dryas Nutrient Stream on North Atlantic Productivity

Finally, we examine paleoclimate records that have been interpreted as indicators of export productivity. These include records of fluxes of organic components to the sediments as well as microfossil assemblages associated with different productivity regimes. Most of the records that resolve the Younger Dryas climate oscillation show decreased productivity relative to the millennia immediately before and after the event (**Fig. 4, Table S1**). While changes in oceanic conditions influencing productivity over the Younger Dryas may have influenced each site differently, the overall reduction of productivity in the region is consistent with the diminished supply of nutrients. This provides observational support of the causal chain inferred from global climate model simulations, that AMOC weakening leads to reduced advective supply of nutrients and declining North Atlantic primary productivity. We also highlight that while North Atlantic primary productivity is expected to decline in the case of either a weakening or collapse in the AMOC, the sign of biogeochemical changes in the intermediate waters of the open ocean North Atlantic will be different. The data for the Younger Dryas are consistent with a weakened rather than a collapsed AMOC. While most climate models suggest a weakening of the AMOC over the coming century, a collapse has not been ruled out (*27, 28*), and it worth noting the non-linear response of some biogeochemical impacts between these two scenarios.

References and Notes

1. J. L. Pelegri, G. T. Csanady, Nutrient transport and mixing in the Gulf-Stream. *Journal of Geophysical Research-Oceans* **96**, 2577-2583 (1991).
2. R. G. Williams *et al.*, Nutrient streams in the North Atlantic: Advective pathways of inorganic and dissolved organic nutrients. *Global Biogeochemical Cycles* **25**, (2011).
3. R. G. Williams, V. Roussenov, M. J. Follows, Nutrient streams and their induction into the mixed layer. *Global Biogeochemical Cycles* **20**, (2006).
4. J. L. Pelegrí, I. Vallès-Casanova, D. Orúe-Echevarría, in *Kuroshio Current: Physical, Biogeochemical, and Ecosystem Dynamics,* T. Nagai, H. Saito, K. Suzuki, M. Takahashi, Eds. (Wiley, American Geophysical Union, 2019), pp. 23-50.
5. D. B. Whitt, in *Kuroshio Current: Physical, Biogeochemical, and Ecosystem Dynamics,* T. Nagai, H. Saito, K. Suzuki, M. Takahashi, Eds. (Wiley, American Geophysical Union, 2019), pp. 51-82.
6. J. B. Palter, M. S. Lozier, On the source of Gulf Stream nutrients. *Journal of Geophysical Research* **113**, (2008).

7. F. Fripiat *et al.*, Nitrogen isotopic constraints on nutrient transport to the upper ocean. *Nature Geoscience* **14**, 855-861 (2021).
8. J. L. Sarmiento, N. Gruber, M. A. Brzezinski, J. P. Dunne, High-latitude controls of thermocline nutrients and low latitude biological productivity. *Nature* **427**, 56-60 (2004).
9. V. Masson-Delmotte *et al.*, Contribution of working group I to the sixth assessment report of the intergovernmental panel on climate change. *Climate Change 2021: The Physical Science Basis*, (2021).
10. M. Steinacher *et al.*, Projected 21st century decrease in marine productivity: a multi-model analysis. *Biogeosciences* **7**, 979-1005 (2010).
11. D. B. Whitt, M. F. Jansen, Slower nutrient stream suppresses Subarctic Atlantic Ocean biological productivity in global warming. *Proc Natl Acad Sci U S A* **117**, 15504-15510 (2020).
12. F. Tagklis, T. Ito, A. Bracco, Modulation of the North Atlantic deoxygenation by the slowdown of the nutrient stream. *Biogeosciences* **17**, 231-244 (2020).
13. M. B. Osman *et al.*, Industrial-era decline in subarctic Atlantic productivity. *Nature* **569**, 551-555 (2019).
14. J. Lynch-Stieglitz, The Atlantic Meridional Overturning Circulation and Abrupt Climate Change. *Ann Rev Mar Sci* **9**, 83-104 (2017).
15. D. C. McCorkle, S. R. Emerson, The Relationship between Pore Water Carbon Isotopic Composition and Bottom Water Oxygen Concentration. *Geochimica Et Cosmochimica Acta* **52**, 1169-1178 (1988).
16. D. C. McCorkle, L. D. Keigwin, B. H. Corliss, S. R. Emerson, The Influence of Microhabitats on the Carbon Isotopic Composition of Deep-Sea Benthic Foraminifera. *Paleoceanography* **5**, 161-185 (1990).
17. B. A. A. Hoogakker, H. Elderfield, G. Schmiedl, I. N. McCave, R. E. M. Rickaby, Glacial–interglacial changes in bottom-water oxygen content on the Portuguese margin. *Nature Geoscience* **8**, 40-43 (2014).
18. P. F. Sexton, R. D. Norris, High latitude regulation of low latitude thermocline ventilation and planktic foraminifer populations across glacial–interglacial cycles. *Earth and Planetary Science Letters* **311**, 69-81 (2011).
19. S. Valley, J. Lynch-Stieglitz, T. M. Marchitto, Timing of Deglacial AMOC Variability From a High-Resolution Seawater Cadmium Reconstruction. *Paleoceanography* **32**, 1195-1203 (2017).
20. S. G. Valley, J. Lynch-Stieglitz, T. M. Marchitto, Intermediate water circulation changes in the Florida Straits from a 35 ka record of Mg/Li-derived temperature and Cd/Ca-derived seawater cadmium. *Earth and Planetary Science Letters* **523**, (2019).
21. C. Waelbroeck *et al.*, Consistently dated Atlantic sediment cores over the last 40 thousand years. *Sci Data* **6**, 165 (2019).
22. J. B. Palter, J. L. Sarmiento, A. Gnanadesikan, J. Simeon, R. D. Slater, Fueling export production: nutrient return pathways from the deep ocean and their dependence on the Meridional Overturning Circulation. *Biogeosciences* **7**, 3549-3568 (2010).
23. D. W. Oppo *et al.*, Data Constraints on Glacial Atlantic Water Mass Geometry and Properties. *Paleoceanogr Paleocl* **33**, 1013-1034 (2018).
24. A. Schmittner, Decline of the marine ecosystem caused by a reduction in the Atlantic overturning circulation. *Nature* **434**, 628-633 (2005).

25. L. Menviel *et al.*, Poorly ventilated deep ocean at the Last Glacial Maximum inferred from carbon isotopes: A data-model comparison study. *Paleoceanography* **32**, 2-17 (2017).
26. S. Gu *et al.*, Assessing the ability of zonal $\delta^{18}O$ contrast in benthic foraminifera to reconstruct deglacial evolution of Atlantic Meridional Overturning Circulation. *Paleoceanogr Paleocl* **34**, 800-812 (2019).
27. W. Liu, S. P. Xie, Z. Y. Liu, J. Zhu, Overlooked possibility of a collapsed Atlantic Meridional Overturning Circulation in warming climate. *Science Advances* **3**, (2017).
28. N. Boers, Observation-based early-warning signals for a collapse of the Atlantic Meridional Overturning Circulation. *Nat Clim Change* **11**, 680-+ (2021).
29. R. Schlitzer, Electronic Atlas of WOCE Hydrographic and Tracer Data Now Available. *Eos Trans. AGU* **81**, 45 (2000).
30. R. Schlitzer. Ocean Data View, https://odv.awi.de (2022).
31. J. Lynch-Stieglitz *et al.*, Muted change in Atlantic overturning circulation over some glacial-aged Heinrich events. *Nature Geoscience* **7**, 144-150 (2014).
32. J. Lynch-Stieglitz, S. G. Valley, M. W. Schmidt, Temperature-dependent ocean–atmosphere equilibration of carbon isotopes in surface and intermediate waters over the deglaciation. *Earth and Planetary Science Letters* **506**, 466-475 (2019).
33. H. Elderfield, R. E. M. Rickaby, Oceanic Cd/P ratio and nutrient utilization in the glacial Southern Ocean. *Nature* **405**, 305-310 (2000).
34. S. P. Bryan, T. M. Marchitto, Testing the utility of paleonutrient proxies Cd/Ca and Zn/Ca in benthic foraminifera from thermocline waters. *Geochem Geophy Geosy* **11**, (2010).
35. G. F. Lutze, H. Thiel, Epibenthic foraminifera from elevated microhabitats; *Cibicidoides wuellerstorfi* and *Planulina ariminensis*. *J Foramin Res* **19**, 153-158 (1989).
36. N. C. Slowey, W. B. Curry, Glacial-Interglacial Differences in Circulation and Carbon Cycling Within the Upper Western North-Atlantic. *Paleoceanography* **10**, 715-732 (1995).
37. E. Geslin, P. Heinz, F. Jorissen, C. Hemleben, Migratory responses of deep-sea benthic foraminifera to variable oxygen conditions: laboratory investigations. *Marine Micropaleontology* **53**, 227-243 (2004).
38. D. C. McCorkle, D. T. Heggie, H. H. Veeh, Glacial and Holocene stable isotope distributions in the southeastern Indian Ocean. *Paleoceanography* **13**, 20-34 (1998).
39. A. W. Jacobel *et al.*, Deep Pacific storage of respired carbon during the last ice age: Perspectives from bottom water oxygen reconstructions. *Quaternary Science Reviews* **230**, (2020).
40. W. Y. Lu, Y. Wang, D. W. Oppo, S. G. Nielsen, K. M. Costa, Comparing paleo-oxygenation proxies (benthic foraminiferal surface porosity, I/Ca, authigenic uranium) on modern sediments and the glacial Arabian Sea. *Geochimica Et Cosmochimica Acta* **331**, 69-85 (2022).
41. J. F. Adkins, K. McIntyre, D. P. Schrag, The salinity, temperature, and delta O-18 of the glacial deep ocean. *Science* **298**, 1769-1773 (2002).
42. M. Siddall *et al.*, Changing influence of Antarctic and Greenlandic temperature records on sea-level over the last glacial cycle. *Quaternary Science Reviews* **29**, 410-423 (2010).
43. O. Duteil *et al.*, A novel estimate of ocean oxygen utilisation points to a reduced rate of respiration in the ocean interior. *Biogeosciences* **10**, 7723-7738 (2013).

44. S. Eggleston, E. D. Galbraith, The devil's in the disequilibrium: multi-component analysis of dissolved carbon and oxygen changes under a broad range of forcings in a general circulation model. *Biogeosciences* **15**, 3761-3777 (2018).
45. L. A. Anderson, J. L. Sarmiento, Redfield Ratios of Remineralization determined by nutrient data-analysis. *Global Biogeochemical Cycles* **8**, 65-80 (1994).
46. T. DeVries, C. Deutsch, Large-scale variations in the stoichiometry of marine organic matter respiration. *Nature Geoscience* **7**, 890-894 (2014).
47. H. E. Garcia *et al.*, "World Ocean Atlas 2018, Volume 3: Dissolved Oxygen, Apparent Oxygen Utilization, and Oxygen Saturation," *NOAA Atlas NESDIS* (2018).
48. H. E. Garcia *et al.*, "World Ocean Atlas 2018, Volume 4: Dissolved Inorganic Nutrients (phosphate, nitrate and nitrate+nitrite, silicate)," *NOAA Atlas NESDIS* (2018).
49. K. Plewa, H. Meggers, S. Kasten, Barium in sediments off northwest Africa: A tracer for paleoproductivity or meltwater events? *Paleoceanography* **21**, n/a-n/a (2006).
50. T. L. Rasmussen, E. Thomsen, S. R. Troelstra, A. Kuijpers, M. A. Prins, Millennial-scale glacial variability versus Holocene stability: changes in planktic and benthic foraminifera faunas and ocean circulation in the North Atlantic during the last 60000 years. *Marine Micropaleontology* **47**, 143-176 (2002).
51. E. Thomas, L. Booth, M. Maslin, N. J. Shackleton, Northeastern Atlantic benthic foraminifera during the last 45,000 years - changes in productivity seen from the bottom up. *Paleoceanography* **10**, 545-562 (1995).
52. J. H. Baas, J. Schonfeld, R. Zahn, Mid-depth oxygen drawdown during Heinrich events: evidence from benthic foraminiferal community structure, trace-fossil tiering, and benthic delta C-13 at the Portuguese Margin. *Marine Geology* **152**, 25-55 (1998).
53. C. Argenio, J. A. Flores, B. Balestra, F. O. Amore, Reconstructing ocean surface dynamics over the last~25 kyr at “Shackleton Site” IODP - U1385. *Palaeogeography, Palaeoclimatology, Palaeoecology* **579**, (2021).
54. B. Ausín, D. A. Hodell, A. Cutmore, T. I. Eglinton, The impact of abrupt deglacial climate variability on productivity and upwelling on the southwestern Iberian margin. *Quaternary Science Reviews* **230**, (2020).
55. E. Salgueiro *et al.*, Past circulation along the western Iberian margin: a time slice vision from the Last Glacial to the Holocene. *Quaternary Science Reviews* **106**, 316-329 (2014).
56. D. Pailler, E. Bard, High frequency palaeoceanographic changes during the past 140 000 yr recorded by the organic matter in sediments of the Iberian Margin. *Palaeogeography Palaeoclimatology Palaeoecology* **181**, 431-452 (2002).
57. N. R. Marshall *et al.*, Biogenic carbonate fluxes and preservation in the northwestern Labrador Sea since the Last Glacial Maximum. *Palaeogeography, Palaeoclimatology, Palaeoecology* **576**, (2021).
58. C. W. Smart, Abyssal NE Atlantic benthic foraminifera during the last 15 kyr: Relation to variations in seasonality of productivity. *Marine Micropaleontology* **69**, 193-211 (2008).
59. N. E. Umling *et al.*, Atlantic Circulation and Ice Sheet Influences on Upper South Atlantic Temperatures During the Last Deglaciation. *Paleoceanogr Paleocl* **34**, 990-1005 (2019).
60. D. W. Oppo *et al.*, Deglacial Temperature and Carbonate Saturation State Variability in the Tropical Atlantic at Antarctic Intermediate Water Depths. *Paleoceanogr Paleocl* **38**, (2023).

61. T. M. Marchitto, W. B. Curry, D. W. Oppo, Millennial-scale changes in North Atlantic circulation since the last glaciation. *Nature* **393**, 557-561 (1998).
62. J. Yu *et al.*, More efficient North Atlantic carbon pump during the Last Glacial Maximum. *Nat Commun* **10**, 2170 (2019).
63. P. Braconnot *et al.*, Results of PMIP2 coupled simulations of the Mid-Holocene and Last Glacial Maximum - Part 2: feedbacks with emphasis on the location of the ITCZ and mid- and high latitudes heat budget. *Clim Past* **3**, 279-296 (2007).

References 32-63 are only called out in the Supplementary Materials.

Acknowledgments: We thank Tiee-Yuh Chiang for her assistance in the laboratory, and two reviewers for their helpful comments which improved the manuscript.

Funding:

National Science Foundation Grant OCE-1459563 (JLS)

National Science Foundation Grant OCE-1851900 (JLS)

Author contributions:

Conceptualization: JLS

Methodology: JLS, SG

Investigation: JLS, TDV, SGV, EB, TMM

Visualization: JLS, SG

Funding acquisition: JLS

Writing – original draft: JLS

Writing – review & editing: JLS, TMM, SG, TDV, SGV

Competing interests: Authors declare that they have no competing interests.

Data and materials availability: All data are available in the supplementary materials. Data are also archived at the NOAA NCEI World Data Center for Paleoclimatology (https://www.ncei.noaa.gov/access/paleo-search/study/38639).

Supplementary Materials

Materials and Methods

Figs. S1 to S4

Tables S1 to S2

References (*28–50*)

Data S1

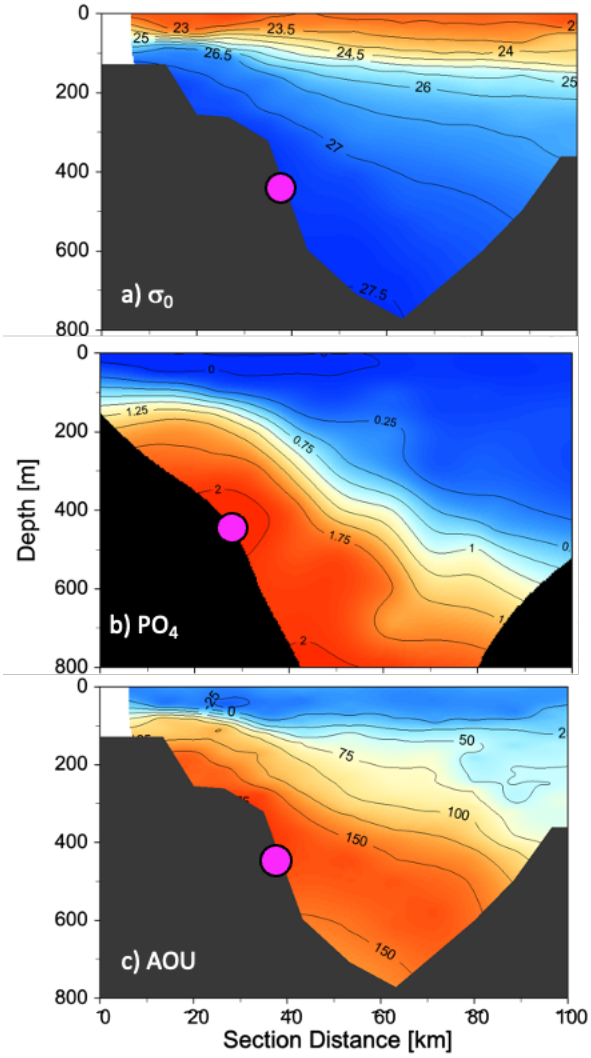

Fig. 1. The nutrient stream in the Florida Straits. The WOCE A5 section across the Florida Current at 26°N from Florida (left) to the Bahamas (right), just downstream of the location of sediment core KNR166-2-26JPC is shown (*29, 30*). a) Potential density (σ_0) kg m^{-3}, b) PO_4 (µmol kg^{-1}), c) AOU (µmol kg^{-1}). The depth of core KNR166-2-26JPC on the Florida Margin is indicated with a magenta circle for all three panels.

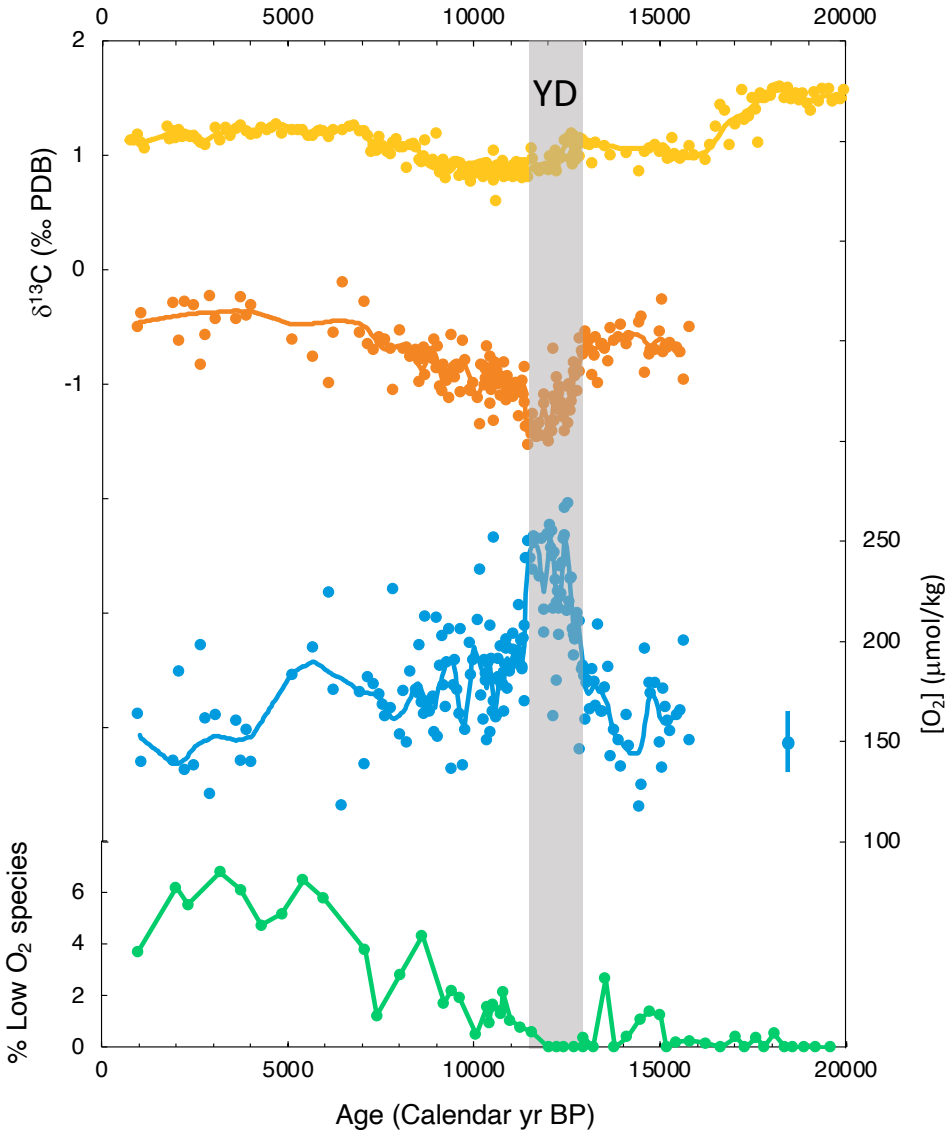

Fig. 2. History of oxygenation in the Florida Straits. The average carbon isotopic composition of tests of the foraminifera *P. ariminensis* (yellow) and *Globulimina* (orange) from KNR166-2-26JPC, and the difference in these values converted to oxygen (blue). The 1-sigma calibration error for the oxygen proxy is indicated in blue. The solid line is a loess smooth through the data. Also shown in green are the proportion of planktonic foraminiferal specimens that are associated with low-oxygen values in the subsurface. The grey bar indicates the Younger Dryas time period.

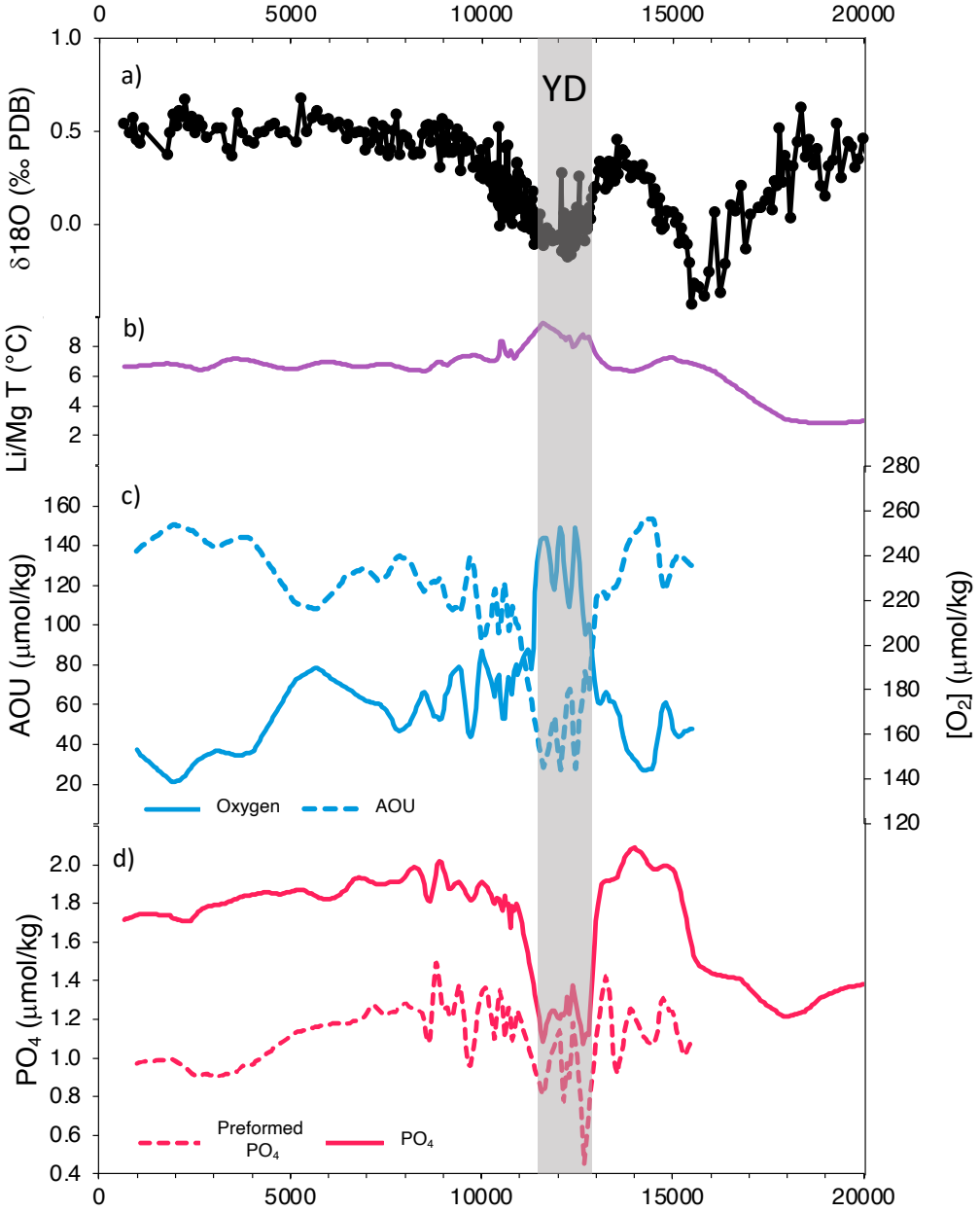

Fig. 3. Florida Straits circulation and biogeochemistry over the deglaciation. a) The ice-volume-corrected oxygen isotope ratio of benthic foraminifera on the Florida Margin at KNR166-2-26PC, which reflects changes in the density contrast across the Florida Straits and the strength of the upper branch of the Atlantic meridional overturning circulation (AMOC) (*14, 26, 31*). b) T estimate from Li/Mg (*20*) c) Smoothed reconstructed oxygen time series as in Figure 3 (solid line), and the Apparent Oxygen Utilization (AOU) based on Li/Mg T reconstruction

(dashed line). d) PO_4 estimated from Cd/Ca ratio (*19*), and preformed PO_4 estimated using AOU. The grey bar indicates the Younger Dryas time period.

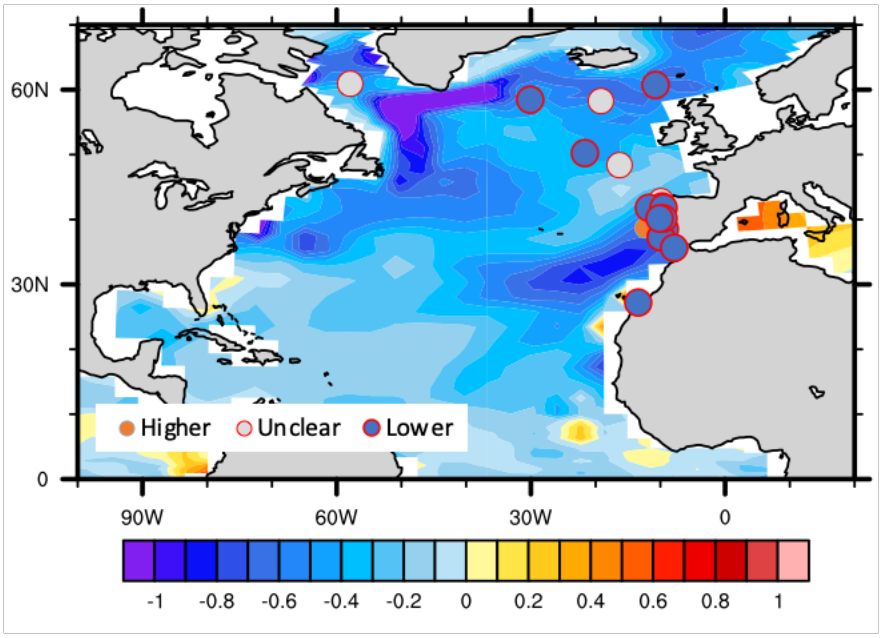

Fig. 4. Younger Dryas productivity anomaly. Circles are sediment core locations where reconstructed productivity is clearly lower than time periods before and after the Younger Dryas (blue), higher than the time periods before or after (orange) or where there is no clear anomaly relative to the time before and after (grey) (**Table S1**). The background is anomaly in the flux of particulate organic carbon (mol m^{-2} yr^{-1}) between a time in the C-iTRACE simulation (*26*) with a weak AMOC (17.5ka) and a strong AMOC (19.5 ka).

Science
AAAS

Supplementary Materials for

A Diminished North Atlantic Nutrient Stream during Younger Dryas Climate Reversal

Jean Lynch-Stieglitz, Tyler D. Vollmer, Shannon G. Valley, Eric Blackmon, Sifan Gu, Thomas M. Marchitto

Corresponding author: jean@eas.gatech.edu

The PDF file includes:

Materials and Methods
Figs. S1 to S4
Tables S1 to S2
References

Other Supplementary Materials for this manuscript include the following:

Data S1

Materials and Methods

Previously Published Age Model and Measurements

We use the age model published by Waelbroeck et al. 2019 (*21*) for JPC26. Stable isotope measurements on *Planulina ariminensis* were published in Lynch-Stieglitz et al. 2014 (*31*) and Lynch-Stieglitz et al. 2019 (*32*). Cd/Ca and Mg/Li measurements on *Hoeglundina elegans* are published in Valley et al. 2017 (*19*) and Valley et al. 2019 (*20*). The calculation of bottom water temperature from Mg/Li and seawater Cd (Cd_w) from Cd/Ca is described in these publications.

Globobulimina Stable Isotope Measurements

The sediment core KNR166-2-26JPC was sampled at 2 cm intervals. Specimens of *Globobulimina* were picked from the >250 μm sieve size fraction. Where available, 5 specimens were analyzed for each sample depth (average number of specimens analyzed per depth was 2.5). Analyzed individuals had a median mass of 43 μg (range 20-219 μg, 96% < 100 μg). Each specimen was photographed before analysis (**Figure S3**) and analyzed individually using a Thermo Kiel IV carbonate preparation device coupled to a MAT253 and calibrated using NBS-19 and NBS-18. The standard deviation (1 sigma) of replicate analyses of an in-house carbonate standard in the 20-100 μg size range analyzed at the same time as the samples was .06 for $\delta^{18}O$ and .03 for $\delta^{13}C$. Measurements with oxygen isotope values that were greater than 2 s.d. away from a robust Loess smoothed version of the record were flagged (4% of the data) and not included in the $\delta^{13}C$ averages calculated for each depth (**Figure S4**)

Determination of Biogeochemical Variables from Proxy Measurements

PO_4

PO_4 was estimated from Cd_w using the relationship described in in Elderfield and Rickaby (*33*) with alpha = 2.5 for the Atlantic Ocean (*34*).

O_2

In situ oxygen concentration is calculated from the difference between the $\delta^{13}C$ of *Globobulimina* and *P. ariminensis* using the relation in Hoogakker et al. (*17*). While this relation was developed using *C. wuellerstorfi*, in this region *C. wuellerstorfi* are not found at the shallow water depths of this core site, but *P. ariminensis*, another elevated epibenthic species (*35*) is abundant and reliably records the $\delta^{13}C$ of seawater (*36*). Where *P. ariminensis* $\delta^{13}C$ was not available at the same depth as the *Globobulimina* $\delta^{13}C$ data, the average $\delta^{13}C$ of *P. ariminensis* from the two depths above and below the sample depth was used. This proxy for past oxygen concentration is based on the assumption that *Globobulimina* records the $\delta^{13}C$ at the depth in the sediments where pore water oxygen goes to zero, that *P. ariminensis* records bottom water $\delta^{13}C$, and that the pore water $\delta^{13}C$ differs from surface water due to the remineralization of organic matter using oxygen supplied by diffusion from above. There is evidence that these assumptions can be violated to some extent in some locations, with observations of deeper depth habitats for *Globobulimina* and evidence for sulfate reduction contributing to the low pore water $\delta^{13}C$, and locations where the proxy doesn't seem to give reasonable values (*37-40*). Despite these complications, $\delta^{13}C$ difference between these species at an increasing number of locations is well correlated to overlying oxygen concentration. At our core site, the reconstructed Holocene values are similar to the modern measurements (150 μM) near this site. The oxygen

reconstruction matches well with the completely independent Cd-based PO_4 reconstruction, also giving us confidence in the application of the proxy at this site.

AOU

Apparent Oxygen Utilization (AOU) is defined to be the difference between O_2 concentration at saturation and the in-situ oxygen concentration. Oxygen at saturation (TEOS-10) is calculated using the Mg/Li derived temperature. Where Mg/Li temperature is not available at the same sample depth as *Globobulimina*, the average Mg/Li T value for the depths above and below is used. While the oxygen saturation changes are dominated by temperature, we adjust the modern salinity value by scaling the glacial-interglacial difference for the North Atlantic measured at Feni Drift of 1.115 (*41*) to global ice volume changes with time (*42*). While we do not adjust for any local changes in salinity, a 1 psu difference in salinity corresponds to only a 2 $\mu mol\ kg^{-1}$ difference in oxygen saturation. Note that AOU may not be the same as the True Oxygen Utilization (TOU), if the seawater water was not saturated with respect to oxygen when it left the surface. Intermediate waters in today's North Atlantic are estimated to leave the surface with an undersaturation of up to 15-20 μM (*43*), and as a result AOU overestimates TOU by a similar amount. The initial disequilibrium in intermediate waters in the North Atlantic may increase to up to 35 μM for cold climates (*44*).

PO_{4pre}

For the depths where both AOU and Cd-based PO_4 estimates are available, preformed PO_4 is calculated using AOU: $PO_{4pre} = PO_4 - (1/170)*AOU$, where 1:170 is the average P:-O_2 ratio of remineralized carbon (*45*). When preformed PO_4 is calculated using AOU, the true preformed PO_4 will be underestimated by a proportionate amount, (AOU-TOU)/170. If the disequilibrium for the deglaciation was in the range of 15-35 μM, this would correspond to an underestimate of true PO_{4pre} by .1-.2 μM. If the degree of disequilibrium changed over the Younger Dryas climate oscillation, this could change the partitioning of the remineralized and preformed changes by a similar amount. The value of P:-O_2 ratio 1:170 from Anderson and Sarmiento (*45*) is widely used in models and data studies, and matches the values for the intermediate Atlantic in more recent studies (*46*). However, these more recent studies suggest a global average ratio of about 1:150. Using this value would reduce P_{pre} for the portion of our record with highest AOU values by about .1 μM, and the qualitative inferences we draw here would not change.

Planktonic Species Counts

Samples were selected for counting to be approximately 300 years apart based on the age model. We isolated portions of each sample from greater than 150 micrometers sieve fraction. We split the samples, and examined a portion which contained a minimum of 300 total planktonic foraminifera. The total number of planktonic foraminifera, *Globorotalia menardii and Globorotalia tumida* (*G. menardii* complex) and *Pullentinia obliquiloculata* were counted. Lastly, prior to this work with the core we had removed *Globogerinoides ruber* from the samples for isotopic analysis and counts of total foraminifera were adjusted to reflect this.

N. Atlantic Productivity Compilation

We examined each productivity record that had at least one Younger Dryas aged data point to see if the Younger Dryas productivity was consistently lower or higher than for the data points immediately before and after the Younger Dryas (**Table S1**). If there was no difference or there

was a change across the Younger Dryas (e.g. Younger Dryas productivity was higher than before the Younger Dryas and lower than after the Younger Dryas), the Younger Dryas productivity anomaly was marked “unclear”. Interpretations of productivity proxies and identification of the Younger Dryas interval were taken as written from the original papers.

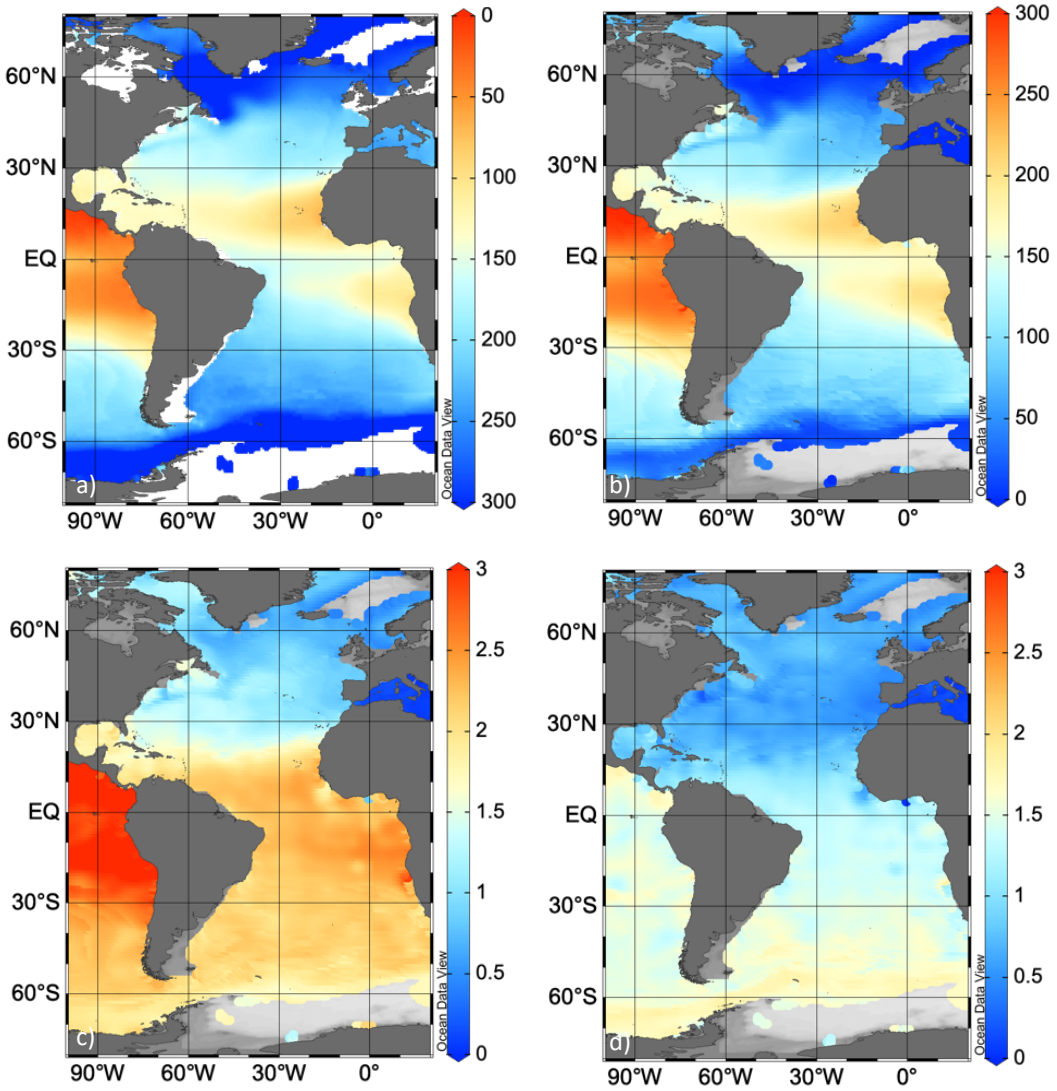

Fig. S1.

Properties along the 27.3 isopycnal from modern climatology (*30, 47, 48*). a) Oxygen (μmol kg^{-1}) b) AOU (μmol kg^{-1}), c) PO_4 (μmol kg^{-1}), d) Preformed PO_4 (μmol kg^{-1}).

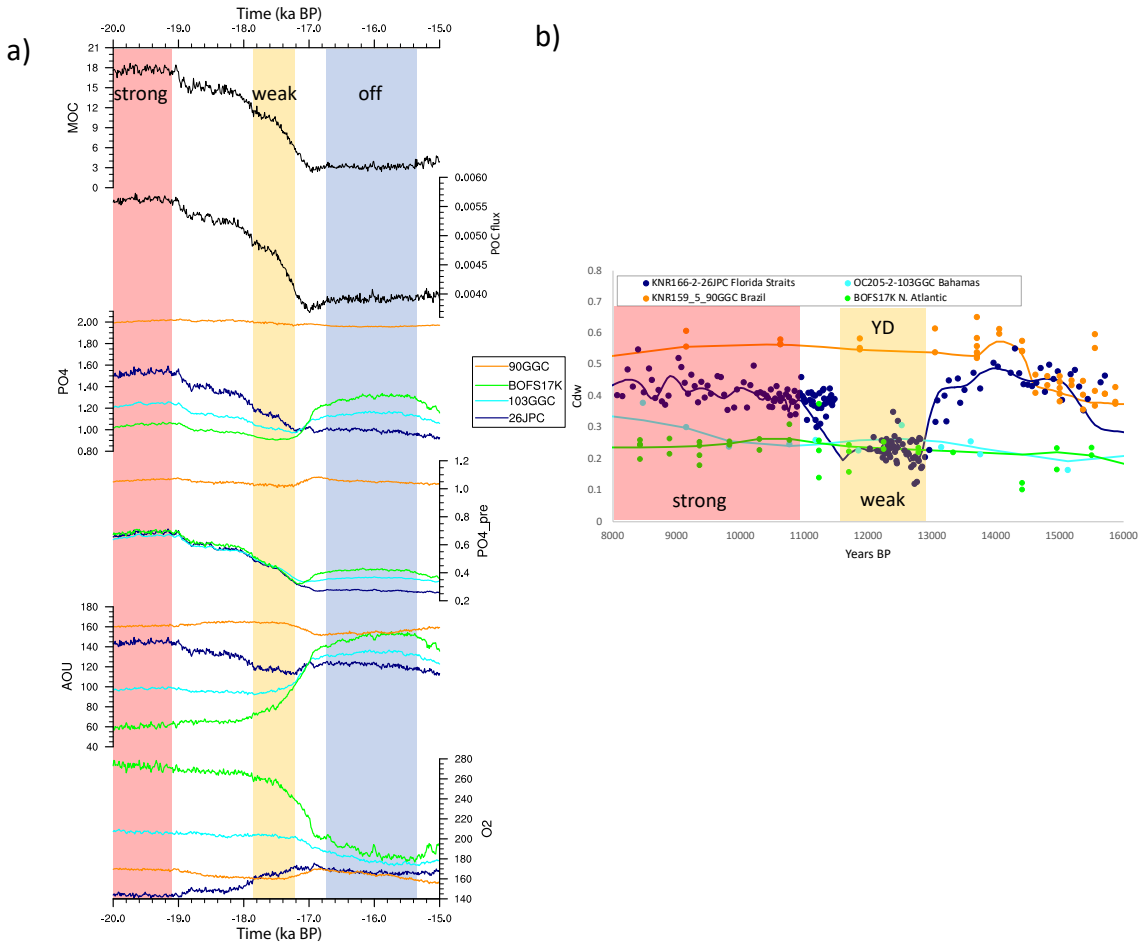

Fig. S2. AMOC strength and regional nutrient patterns. (a) Time series of AMOC, North Atlantic productivity (averaged over domain shown in Figure 4), and biogeochemical properties from the C-iTRACE simulations between 20 and 15ka (*26*). Properties are shown at core sites where nutrient reconstructions are available over the Younger Dryas P_{pre} is calculated using AOU, in the same way as for the proxy reconstructions. In the model, a weaker AMOC ("weak") is accompanied by lower PO_4, P_{pre}, AOU, and higher O_2 at the Florida Straits (dark blue) than for the time when AMOC is strong ("strong"). However, for the open ocean N. Atlantic intermediate water sites (green and light blue), when the AMOC collapses ("off"), nutrient concentrations and AOU increase to levels higher than seen in the intermediate waters in the Florida Straits. (b) Reconstructions of seawater Cd_w, a proxy for PO_4 over the Younger Dryas. Intermediate water Cd_w remain high in the South Atlantic, and low in the North Atlantic over the entire time period. Florida Straits values converge towards N. Atlantic values during the Younger Dryas as is seen during times of moderate AMOC weakening in the model ("weak"). Locations, depths, and modern density for the core sites shown are in **Table S2**.

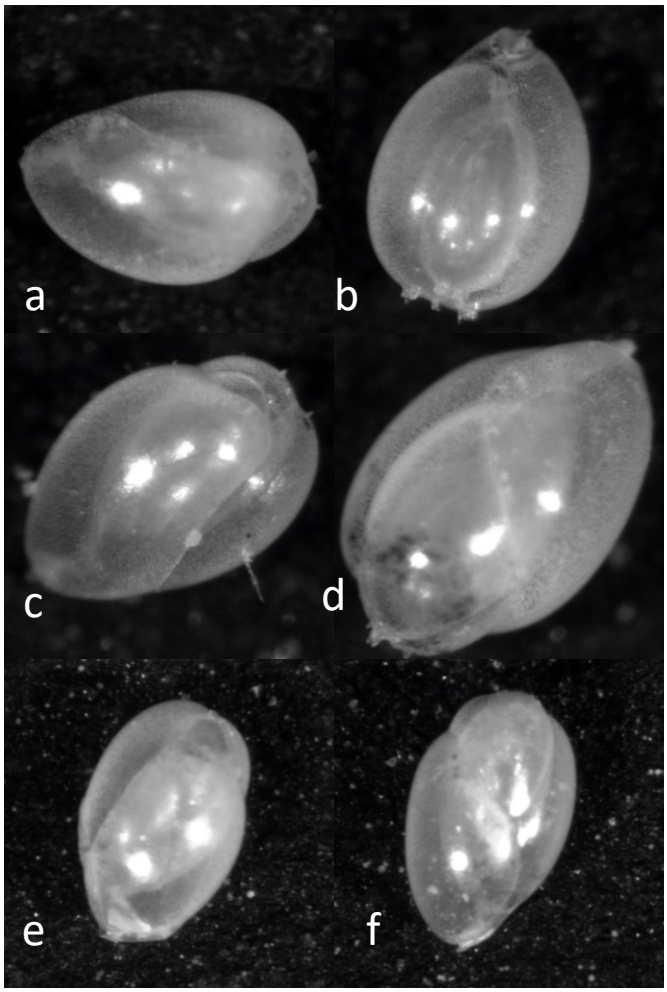

Fig. S3. Example specimens of benthic foraminifera. *Globobulimina* from KNR166-2-26JPC, depth in core and mass of test indicated for each: a) 206 cm 36 µg b) 206 cm 44 µg, c) 404 cm 44 µg d) 404 cm 89 µg, e) 686 cm 25 µg, f) 686 cm 25 µg

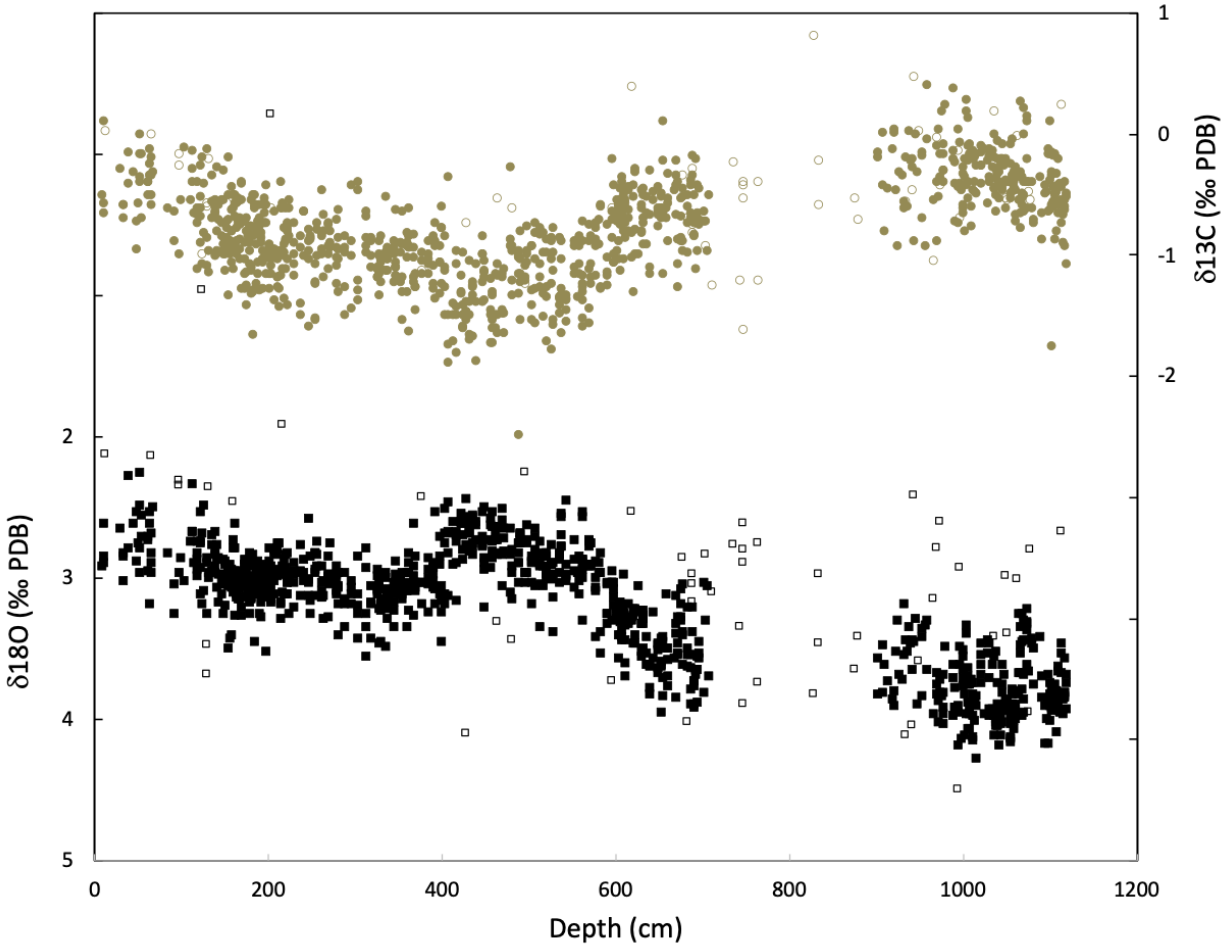

Fig. S4. Individual Globobulimina carbon and oxygen isotope measurements vs. core depth. Light symbols indicate individuals that were not included in the average $\delta^{13}C$ value for each depth.

Core	Latitude (°N)	Longitude (°E)	Younger Dryas Productivity	Productivity Proxy	Reference
GeoB5546-2	27.5	-13.7	low	organic carbon	(*49*)
DS97-2P	58.9	-30.4	low	foram accum rates	(*50*)
ENAM33	61.3	-11.1	low	foram accum rates	(*50*)
BOFS 5K	50.7	-21.9	low	benthic foram assemblage	(*51*)
SO75-26KL	38.8	-9.5	low	organic carbon	(*52*)
U1385	37.6	-10.1	low	nannofossil abundance	(*53*)
SHAK06-5K	37.6	-10.2	low	nannofossil abundance	(*54*)
OMEXII-9K	42.3	-10.1	low	planktonic assemblage	(*55*)
N3KF24	42.1	-12.0	low	planktonic assemblage	(*55*)
MD03-2697/MD99-2331	42.2	-9.7	low	planktonic assemblage	(*55*)
MD95-2040	40.6	-9.9	low	planktonic assemblage	(*55*)
MD95-2039	40.6	-10.4	low	planktonic assemblage	(*55*)
M39029-7	36.1	-8.2	low	planktonic assemblage	(*55*)
BOFS 14K	58.6	-19.4	unclear	benthic foraminifera	(*51*)
MD952042	37.8	-10.2	unclear	C37 mass accumulation rate	(*56*)
PO200-10-26-2	41.5	-9.7	unclear	organic carbon	(*52*)
HU2008–029-004	61.5	-58.0	unclear	multiproxy biogenic fluxes	(*57*)
SU92-03	43.2	-10.1	unclear	planktonic assemblage	(*55*)
OMEXII-5K	41.8	-10.0	unclear	planktonic assemblage	(*55*)
MD95-2042	37.8	-10.2	unclear	planktonic assemblage	(*55*)
BENGAL 13078#16	48.8	-16.5	unclear	benthic foraminifera	(*58*)
MD01-2446	39.1	-12.6	high	planktonic assemblage	(*55*)
MD99-2339	35.9	-7.5	high	planktonic assemblage	(*55*)

Table S1. Productivity records shown in Fig. 4

Core	Latitude (°N)	Longitude (°E)	Depth (m)	Modern σ_t	Reference
KNR159-5-90GGC	-27.4	-46.6	1108	27.3	(*59, 60*)
KNR166-2-26JPC	24.3	-82.3	546	27.3	(*19*)
OCE205-2-103GGC	26.1	-78.1	965	27.6	(*61*)
BOFS17K	58.0	-16.5	1150	27.6	(*62, 63*)

Table S2. Cd Records shown in Fig. S2

Data S1. (separate file)

An excel file containing measured and derived variables. Data are also be archived at the World Data Center for Paleoclimatology.